JOURNAL OF MATERIALS SCIENCE 15 (1980) 119–126

δ-FeO(OH) and its solid solutions

Part 2 *High resolution transmission electron microscopy of pure δ-FeO(OH)*

WILLIAM KRAKOW*, HENDRIK COLIJN, OLAF MULLER
Xerox Corporation, Xerox Square W114, Rochester, New York 14644, USA

A transmission electron microscope imaging investigation was performed on small δ-FeO(OH) crystallites less than 50 Å thick and several hundred angstroms across. We have observed faceting, and a hexagonal plate-like morphology with topological features near atomic step heights. Because of the mutual magnetic attraction on these particles, they tend to align with their thin direction (*c*-axis) either parallel or perpendicular to the support film surface. It is therefore possible to view dislocations or buckling of lattice planes of these plates either edge-on or perpendicular to this direction by direct lattice imaging in both the bright-field and dark-field modes. A highly distorted lattice is apparent when viewing the particles edge-on, and it is possible to show lattice projections to a resolution of 2.1 Å.

1. Introduction

In the first paper in this series (Part 1 [15]) the preparation and crystal chemistry of δ-FeO(OH)-type solid solutions was discussed, and a structural model was postulated for phases of the type $Fe_{1-x}Zn_xO_{1-x}(OH)_{1+x}$ for x up to 0.40. The structure of pure δ-FeO(OH) has only been determined to a rough approximation by Okamoto [1]. Therefore, this paper deals with the structural and morphological characteristics of the unsubstituted δ-FeO(OH) phase which was investigated by high-resolution transmission electron microscopy (TEM). A third investigation will deal with an X-ray diffraction and electron microscope study of the thermal decomposition of $Fe_{1-x}M_xO_{1-x}(OH)_{1+x}$ type materials. A final paper will deal with their magnetic properties.

Up to the present, there have been few electron microscopic studies to determine morphological and structural information about δ-FeO(OH). Okamoto [2, 3] has shown several low-magnification bright-field micrographs of δ-FeO(OH) prepared using various concentrations of NaOH. He found that the particle size increased with increasing NaOH concentration [3]. His results, however, are mainly concerned with particle size analysis and hence did not require any detailed electron microscope imaging studies. Similar electron microscope investigations have been performed using relatively low microscope magnifications to observe the shape and size of ferric oxyhydroxide particles [4–6], i.e. α, β, γ and δ-FeO(OH) phases formed under various conditions, as well as their changes induced under various heat-treatments.

The topotactic oxidation $Fe(OH)_2 \rightarrow$ δ-FeO(OH) described in Part 1 has its counterpart in the topotactic oxidation of $Mn(OH)_2$ to β-MnO(OH)†. This latter transformation has been studied by Oswald *et al.* [7] using TEM at a somewhat higher resolution than the investigations mentioned above and by electron diffraction. The images of the hexagonal platelets of β-MnO(OH) revealed a mottled appearance down to dimensions of 15 Å, the limit of the resolution in their microscope.

*Present address: IBM Corporation, Thomas J. Watson Research Center, P.O. Box 218, Yorktown Heights, New York 10598, USA.

†$Mn(OH)_2$ and $Fe(OH)_2$ have the same structure, although β-MnO(OH) and δ-FeO(OH) do not.

0022–2461/80/010119–08$02.80/0

Very high-resolution microscopy has been used infrequently to investigate the oxyhydroxides of iron. One study used bright-field lattice imaging to characterize α, β and γ-FeO(OH) and explore the morphological aspects and their reaction with silica [8]. The lattice images in this case sufficed to confirm the expected spacings for the unreacted FeO(OH) polymorphs, showing no detectable uptake of silica.

Another study of a hydrated ferric hydroxide was an investigation using high-resolution dark-field electron microscopy by Massover and Cowley [9]. This "mineral" is part of the iron storage protein, ferritin, and is located within the central cavity of a protein complex. Here the authors have observed regular planar spacings between 2.2 and 9.5 Å in crystallites which are 50 to 75 Å in diameter. Their findings are in accord with a variable iron occupancy model of ferric ions in certain planes of the lattice consistent with a postulated model of Towe and Bradley [10].

In view of the limited number of investigations mentioned above, we have studied δ-FeO(OH) using high-resolution transmission electron microscope techniques. Emphasis was placed on investigating morphological features which include: surface roughness, particle thickness, faceting, and particle aggregation, as well as lattice distortions and imperfections.

2. Experimental procedures

The procedure for the chemical preparation of δ-FeO(OH) powders has been described in Part 1 and will not be repeated here. Since the main interest of the present paper is high-resolution microscopy of these submicron particles, a description of the specimen mounting techniques and instrumental parameters will be presented.

All the transmission electron microscope investigations were performed in a Siemens Elmiskop 102 microscope at 125 kV with an objective lens spherical aberration coefficient of $C_s = 1.9$ mm. For tilted beam dark-field imaging a 30 μm objective aperture was employed with an angular acceptance of ~ 0.018 rad. which provided a maximum resolution of ~ 2 Å. For selected-area electron diffraction (SAD) experiments from single δ-FeO(OH) particles a 10 μm field-limiting aperture was utilized to sample areas of ~ 0.2 μm diameter on the specimen. Diameters five times this size were used to sample fields of particles for SAD powder pattern data. Note that electron beam currents of 1 to 10 A cm^{-2} were used to illuminate the specimen for dark-field microscopy with typical exposure times for dark-field images being from 4 to 8 sec at × 300 000 to × 500 000 magnifications. This amount of intensity usually was not sufficient to convert δ-FeO(OH) to α-Fe_2O_3 as is readily observed from electron diffraction data.

Specimen preparation for microscopy consisted of ultrasonic agitation of the powders in ethanol and subsequent dispersal on ~ 50 Å thick carbon films prepared by indirect vapour deposition from a carbon arc. The purpose of using such thin films was to minimize the background image contribution of the support film for dark-field imaging. This allowed the direct observation of the planar spacings of these plate-like particles for a variety of crystallographic orientations. In other instances reticulated carbon films were employed and particles were sought which were partially suspended over the holes, thus achieving an effect similar to the thin carbon films.

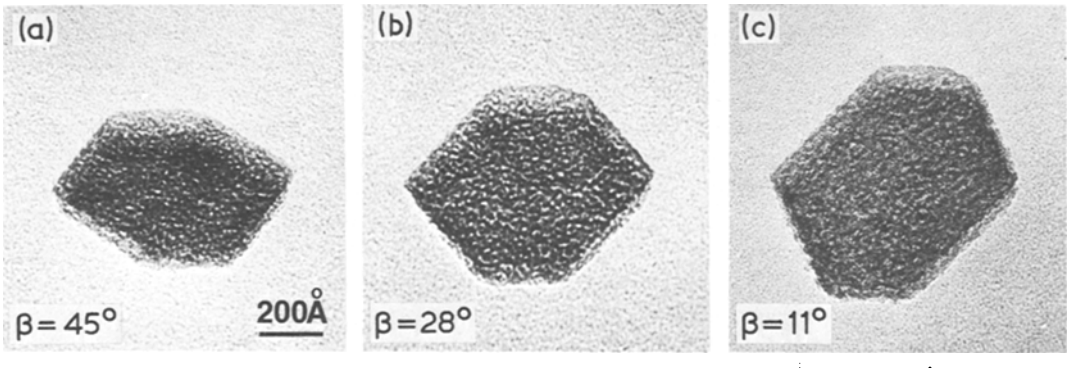

Figure 1 Bright-field images of an inclined δ-FeO(OH) particle on a carbon substrate. Using a $x-y$ goniometer stage, one tilt axis was 45° and the others corresponded to (a) 45°, (b) 28° and (c) 11°.

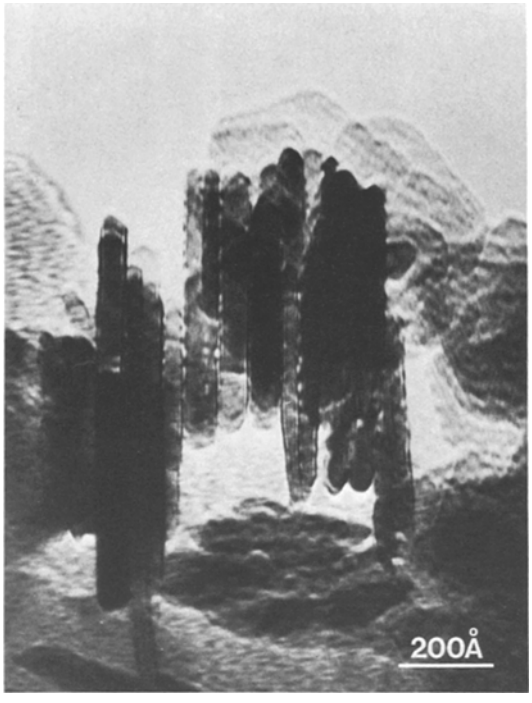

Figure 2 Edge on view of δ-FeO (OH) showing face-to-face coupling of particles using bright-field axial illumination.

3. Results and discussion

Several structural features of pure δ-FeO(OH) were observed in the imaging mode, such as faceting, topological features, mutual magnetic adhesion, dislocations, and lattice planes. We will not consider single crystal electron diffraction data in this publication since it is straight-forward and is best considered in the context of substitutional decomposition products, the subject of the third paper in this series.

3.1. Particle shape and size

The general morphology of the δ-FeO(OH) particles is revealed in Fig. 1 where several views or inclinations of a particle lying flat on a carbon film are revealed. Here we used a microscope x–y goniometer stage which was capable of 45° tilt about either orthogonal axis giving a maximum tilt inclination of 54°. One of the tilt inclinations was kept constant at 45° and the second varied as indicated below each figure by its corresponding β value (45°, 28°, 11°). It is apparent that there are edge features or facets which are visible in projection and change as a function of particle inclination. In general, many of the particles observed for the pure δ-FeO(OH) showed a well-formed hexagonal plate-like morphology. The thin direction of individual particles was found to correspond to the c-axis of the δ structure.

When the particles were dispersed on thin carbon films a substantial number were found to agglomerate with their c-axes being parallel to the support film surface which enabled the viewing of the particles edge-on as demonstrated in Fig. 2. Here individual crystallites appear to adhere to each other either by electrostatic or magnetic forces. There seems to be face-to-face aggregation of the platelets in this case when ethanol is the dispersing medium. This differs from dispersion in water as reported by Powers [11] which appeared to produce chain-like aggregation with no face-to-face contact.

It is interesting to note the dark fringe-like patterns at the edge of each particle in Fig. 2. These features are believed to be caused by Fresnel diffraction from a straight edge. This effect is due to the range of defocus values over which the

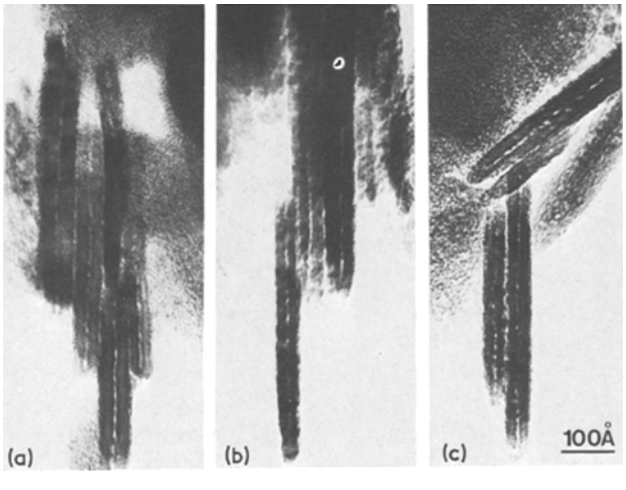

Figure 3 Bright-field images of paired δ-FeOOH particles viewed edge-on

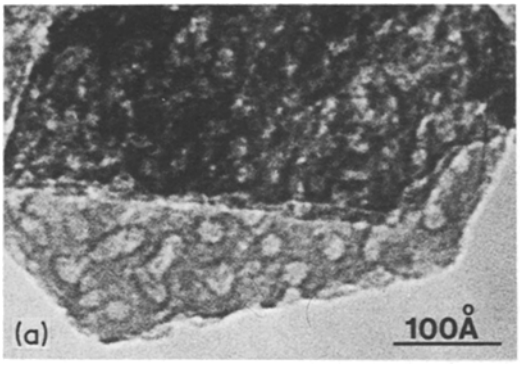

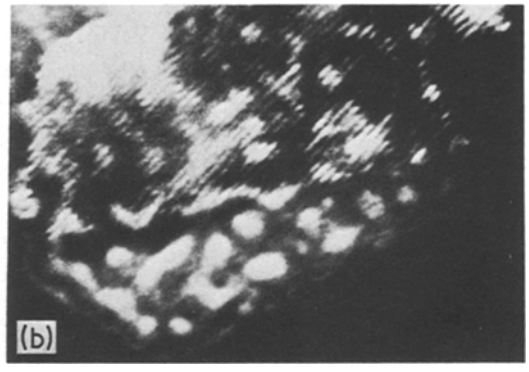

Figure 4 Surface topographical features of a δ-FeO(OH) plate in (a) bright-field axial illumination, (b) and (c) tilted beam dark-field images from different reciprocal space regions.

particles can be visualized edge-on, and it was found that this feature could be eliminated under the proper defocus conditions. Often, evidence for the apparent pairing of particles was found when they were viewed edge-on. Three examples of this pairing are shown in Fig. 3 where there is a white line separating the two components. The most likely explanation for this feature is a cementation process which has already been postulated by Powers [11] to explain his observation that the $Fe(OH)_2$ precursor platelets increase in average particle diameter during ageing in contact with the supernatent alkali solution. After precipitation with excess alkali, the initially formed $Fe(OH)_2$ particles cannot grow rapidly via the solvent medium due to the very low iron concentration in the NaOH solution. Powers observed that the particle growth continues for at least 20 min and postulated that a cementation process must operate to account for this rapid growth. Since our $Fe(OH)_2$ precursor particles were similarly aged for several minutes before being oxidized, a similar cementation process would be expected (see Part 1 for the method of preparation [15]). The {0 0 1} faces of the hexagonal platelets are obviously the most likely sites for such a process since individual crystallites with only a few unit cells along the *c*-direction would be expected to be inherently unstable. Thus the cementation into paired platelets is not surprising. From Fig. 3 it appears that in some platelet pairs the ends of the crystal have intergrown more intimately than the central part, giving the appearance of a hinge. The vertically stacked crystallites in Fig. 2 may also have undergone partial cementation, although this is not as obvious as in Fig. 3. Such a cementation was not observed in the TEM micrographs of Powers [11] due to the lower magnification and lack of micrographs of particles stacked edge-on.

3.2. Surface topography

As shown in Fig. 4, when visualizing δ-FeO(OH) plates along the *c*-axis, thickness variations appear as small patches < 50 Å across. These are presumably of atomic step height or a small integral multiple of this dimension, since the total plate thickness rarely exceeds a few tens of angstroms. The origin of these thickness variations can be explained by the volume contraction which accompanies the violent transformation from $Fe(OH)_2$ to δ-FeO(OH) via a peroxide treatment. Based upon unit cell dimensions from the JCPDS card tables, this contraction is 20%. Discounting the overlap region in the micrograph displayed in Fig. 4a, the surface area of the lighter regions corresponds to 40 to 50% of the total particle area in projection. One can speculate that the sharper features may be surface craters, while other patches may be inclusions deeper within the crystallite. Taken together, such patches could account for the expected 20% shrinkage. Some of the surface roughness seen in Fig. 3 may also

be due to surface craters, although such features are less obvious since they are seen edge-on together with more elevated ridges. The same type of monolayer surface structure was observed by Iijima for very thin graphite films using bright-field imaging [12]. He observed very small holes that were formed at the surface and grew as atomic steps under intense electron beam irradiation. This may be similar to the $Fe(OH)_2$ case where a catastrophic collapse or contraction of the structure occurs by rearrangement of Fe atoms and the net loss of an H^+ ion. In the δ-structure, both the (0 0 0) and (0 0 $\frac{1}{2}$) sites are fractionally occupied by Fe. It is probable that the Fe occupation on these sites is not statistical over a very small area ($\sim 20\,Å^2$) but that Fe-rich regions alternate with clusters of vacancies. This can lead to modified structure factors in localized areas of a δ-FeO(OH) crystallite*. The surface topography and clustering of Fe^{3+} ions within the partially occupied sites can be observed by using dark-field microscopy by sampling different regions of reciprocal space as shown in Fig. 4b and c. Discounting the Moiré effect of particle overlap, some regions in Fig. 4b are diffracting strongly, and a close match with the light patches in Fig. 4a is evident. The same area is shown in Fig. 4c, but with a different sampling of reciprocal space; here the bright regions occur in different locations, frequently in areas which were dark in Fig. 4b. The patchy appearance shown in Fig. 4 is not likely to be a consequence of intense electron beam bombardment since the same phenomenon can be observed under both low beam-dose bright-field imaging and more intense dark-field illumination conditions.

Returning to Fig. 4a the possibility must also be considered that the bright patches may be due to the formation of volatiles as opposed to simple volume contraction during the topotactic $Fe(OH)_2 \rightarrow \delta$-FeO(OH) conversion with H_2O_2. It has been postulated [3] that this conversion involves the migration of H^+ and e^- to the surface of the crystal where the hydrogen combines with oxygen (from the decomposition of H_2O_2) to form water. This sudden and strong reaction involves a great deal of heat and could contribute to the formation of surface craters in areas where the hydrogen evolves and combines with the oxygen. If some of the active oxygen (liberated from the decomposition of H_2O_2) penetrated the layers of the $Fe(OH)_2$ crystallites† the hydrogen and oxygen could combine inside the crystal causing local disruptions in the atomic order and a local recrystallization with the formation of larger voids, i.e. clusters of vancancies. If this is true, the final overall δ-structure can be likened to Swiss cheese with the Fe atom clusters ending up in both the (0 0 0) and (0 0 $\frac{1}{2}$) sites.

The above analysis is in general agreement with the findings of Okamoto [3] who found from half-width X-ray diffraction analysis that the line broadening in $Fe(OH)_2$ is caused only by the small size whereas in the δ-structure it is attributed to both small size and imperfect crystallinity. Our findings are not in conflict with Okamoto's [3] observation that the overall particle size and shape does not change in going from $Fe(OH)_2$ to δ-FeO(OH).

3.3. Lattice images and defects

In addition to investigating general morphological features observed in δ-FeO(OH) particles, it is possible to obtain very high-resolution bright-field and dark-field images showing lattice periodicities and imperfections.

Lattice planes can be imaged indirectly when particles are lying on a film surface since there is considerable overlap leading to Moiré patterns as demonstrated in Fig. 5. The region which has horizontal fringes required only a moderate level of resolution (~ 12 Å fringes) as is shown in an enlarged view in the accompanying insert. Here

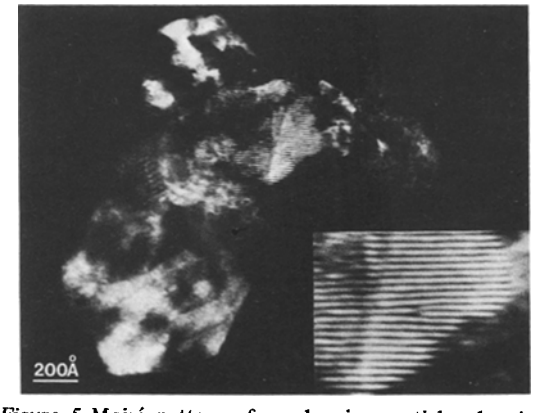

Figure 5 Moiré pattern of overlapping particles showing an edge dislocation.

*A discussion of partially filled unit cells can be found in [13] and [14].

†The anion layers in $Fe(OH)_2$ (CdI_2 structure) are held together only by weak forces since there are no cations in the (0 0 $\frac{1}{2}$) position, and here the structure could be easily penetrated by active oxygen.

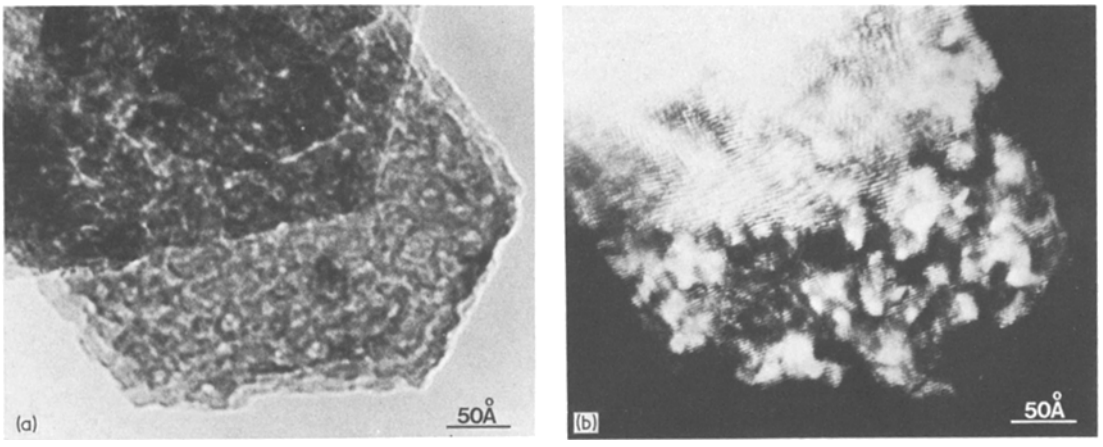

Figure 6 Images of a δ-FeO(OH) plate. (a) bright-field image, (b) tilted beam dark-field lattice image of {1 0 0} type lattice planes.

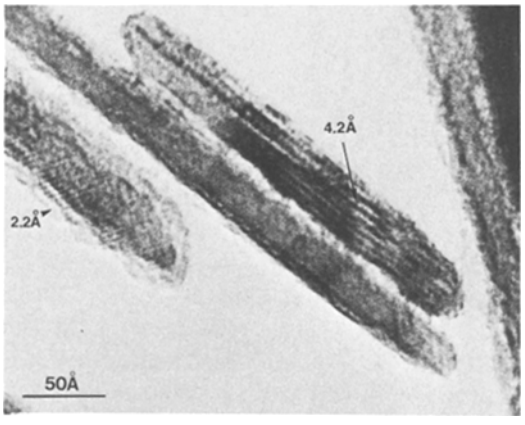

Figure 7 Bright-field edge on view of δ-FeO(OH) showing faceting and both the (0 0 1) and (1 0 1) lattice planes.

it is apparent that an edge dislocation type defect is present.

At higher resolutions it is possible to image directly lattice planes of crystallites lying flat on the film surface, i.e., along the δ-FeO(OH) *c*-axis direction. This result is shown in Fig. 6 where (a) is a bright-field axial illumination image showing general particle morphology and (b) is a dark-field lattice image of the same particle showing both the (1 0 0) and (0 1 0) lattice fringes of 2.5 Å. In (a) the microscope resolution at 125 kV was not sufficient to visualize the 2.5 Å periods but it can be seen that a large region of the crystal is not overlapped by other adjacent particles. Here the microscope objective lens defocus was not optimized for revealing the surface steps as in Fig. 4. In the complementary dark-field picture in Fig. 6b, the {1 0 0} type lattice images appear in small bright patches. The disorder between these bright regions can best be seen by looking along the length of these fringes at a glancing angle where bending and buckling of the fringes is evident as is considerable planar mismatch between adjacent regions. Such defects are entirely compatible with the postulated $Fe(OH)_2 \rightarrow$ δ-FeO(OH) conversion discussed above.

For particles viewed edge-on it is also possible to observe atomic lattice planes and edge faceting in individual crystals as shown in the bright-field micrograph of Fig. 7. The (0 0 1) lattice periodicity of 4.2 Å‡ is visible and there are facets at the ends of the particle which have been measured to correspond to angular inclinations of 41° and 60° and hence correspond to planar faces of the (1 0 2) and (1 0 1) type, respectively. The dark band visible in one portion of the particle is also believed to be a faceting feature. Here we are looking through perhaps 100 to 200 Å thickness of crystal, and extinction effects related to thickness variations of the faceting could produce this contrast effect. It is also obvious that the 4.2 Å lattice planes are distorted. A second particle in this field of view shows faint (1 0 1) lattice fringes corresponding to a planar spacing of 2.2 Å.

Usually the edge-on views of particles in the bright-field imaging mode are of relatively low contrast and are difficult to observe directly on the microscope viewing screen. By using tilted beam dark-field imaging it is possible to enhance a particle's contrast as demonstrated in Figs. 8 and 9. Here edge faceting is difficult to observe with the lattice distortions being more apparent.

‡The measured 4.2 Å distance corresponds closely to the 4.49 Å c_0-parameter.

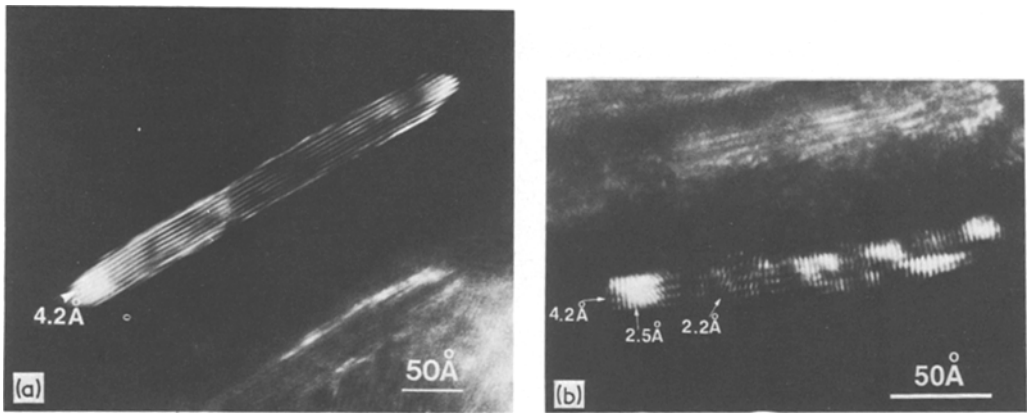

Figure 8 Dark-field images of a δ particle (a) showing the (0 0 1) lattice periodicity. (b) showing the (0 0 1), (1 0 0) and (1 0 1) lattice spacings of 4.2, 2.5 and 2.2 Å, respectively.

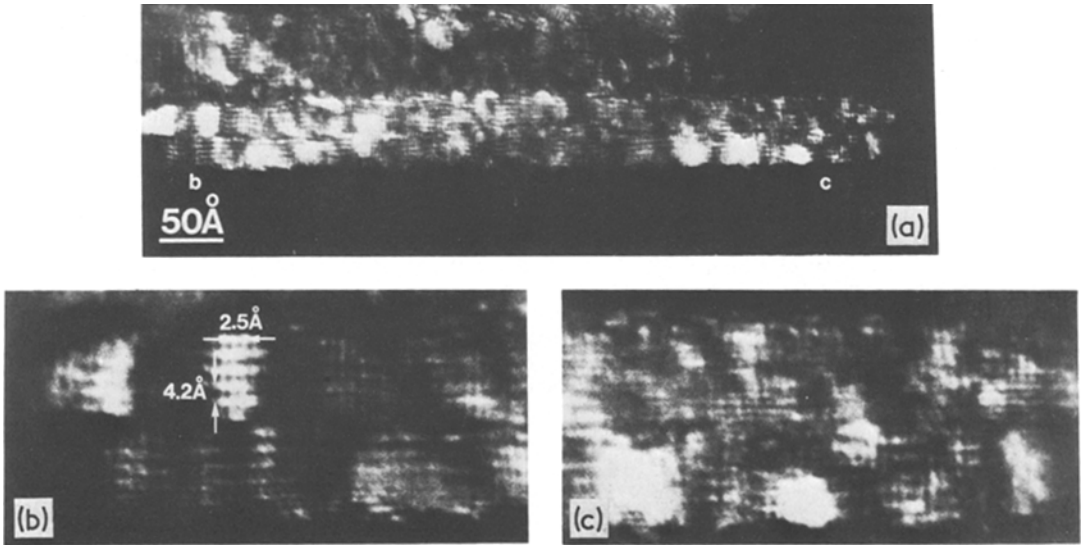

Figure 9 (a) Dark-field image of a δ particle viewed edge-on showing lattice distortions on the (0 0 1) planes. (b) and (c) higher magnifications of indicated areas of image (a).

In Fig. 8a the (0 0 1) lattice plane image has been optimized revealing the 4.2 Å periodicity as well as the bending of the planes. Here there are perceptible faceting features at both ends of the particle. Fig. 8b shows a particle with the (0 0 1), (1 0 0) and at least two (1 0 1) planar periodicities. One interesting feature of this image is at the right side of this particle where the 2.5 Å lattice periods have an abrupt shift in position. It is possible that two separate crystals have been atomically cemented together on the left with each being no more than 2 or 3 unit cell dimensions thick. At the right side, this cementation process has not gone to completion, as seen by the mismatch of the atomic planes.

A final example of dark-field lattice imaging of δ-FeO(OH) particles viewed edge-on is shown in Fig. 9. Two separate particles are in contact and probably cemented together. Note in the higher magnification pictures (b) and (c) of image (a) that weaker periodicities occur along the [0 0 1] direction, corresponding to 2.1 Å, i.e. (0 0 2) spacings or half the c_0-cell dimension. Again it is apparent that the lattice planes are highly distorted, and in fact some regions show a pairing of lines running perpendicular to the thin direction. This latter feature as yet has not been explained, but we speculate that it is due to the partitioning of Fe^{3+} ions between the (0 0 0) and (0 0 $\frac{1}{2}$) sites induced by the rapid $Fe(OH)_2 \rightarrow$ δ-FeO(OH) conversion with H_2O_2.

4. Conclusions

A high-resolution electron microscope analysis of pure δ-FeO(OH) particles has shown that they have a hexagonal plate-like morphology with the thin dimension being at most a few tens of angstroms across. There is evidence of faceting of these particles near an atomic level and for alignment of these superparamagnetic particles face to face. There also appears to be a pairing of crystallites which is due to a cementation process.

Small patches (< 50 Å) visible on the particle surface can be explained as surface craters and/or inclusions caused by the conversion and contraction of the $Fe(OH)_2$ lattice to δ-FeO(OH). The proposed reaction mechanism is compatible with previous structural studies (see Part 1 [15]) and with the findings of Okamoto [3] and Powers [11]. Lattice imperfections are revealed near the atomic level by means of bright-field and dark-field lattice imaging or Moiré patterns with the hexagonal crystals viewed either edge-on or perpendicular to the plate surface.

References

1. S. OKAMOTO, *J. Amer. Ceram. Soc.* 51 (1968) 594.
2. *Idem, J. Chem. Soc. Japan* 67 (1964) 1845.
3. *Idem, ibid* 67 (1964) 1850.
4. W. FEITKNECHT, *Z. Electrochem.* 63 (1959) 34.
5. G. V. LOSEVA and N. V. MARASHKO, *Inorg. Mat.* 8 (1972) 423.
6. W. FEITKNECHT, R. GIOVANOLI, W. MICHAELIS and M. MÜLLER, *Helvetica Chim. Acta* 56 (1973) 2847.
7. H. R. OSWALD, W. FEITKNECHT and P. BRUNNER, "From Molecule to Cell: Symposium on Electron Microscopy", Modena, April 1963, edited by P. Buffa (CNR, Rome, 1964) p. 141.
8. T. BAIRD, J. R. FRYER and S. T. GALBRAITH, *Inst. Phys. Conf. Ser.* 36 (1977) 211.
9. W. H. MASSOVER and J. M. COWLEY, *Proc. Nat. Acad. Sci. USA* 70 (II) (1973) 3847.
10. K. M. TOWE and W. F. BRADLEY, *J. Colloid Interface Sci.* 24 (1967) 384.
11. D. A. POWERS, Ph.D. Thesis, California Institute of Technology (1975).
12. S. IIJIMA, *Optik* 47 (1977) 437.
13. W. KRAKOW and D. G. AST, *Surface Sci.* 58 (1976) 485.
14. W. KRAKOW, *Ultramicroscopy* 4 (1979) 55.
15. O. MULLER, R. WILSON and W. KRAKOW, *J. Mater. Sci.* 14 (1979) 2929.

Received 26th April and accepted 17 May 1979.